

# Parton Densities and Saturation Scale from Non-Linear Evolution in DIS on Nuclei

E. Levin\* <sup>a)</sup> and M. Lublinsky<sup>†</sup> <sup>b)</sup>

*a) HEP Department*

*School of Physics and Astronomy*

*Raymond and Beverly Sackler Faculty of Exact Science*

*Tel Aviv University, Tel Aviv, 69978, ISRAEL*

*b) Department of Physics*

*Technion – Israel Institute of Technology*

*Haifa 32000, ISRAEL*

October 22, 2018

## Abstract

We present the numerical solution of the non-linear evolution equation for DIS on nuclei for  $x = 10^{-2} \div 10^{-7}$ . We demonstrate that the solution to the non-linear evolution equation is quite different from the Glauber - Mueller formula which was used as the initial condition for the equation.

We illustrate the energy profit for performing DIS experiments on nuclei. However, it turns out that the gain is quite modest:  $x_{Au} \simeq 5 x_{\text{proton}}$  for the same parton density.

We find that the saturation scale  $Q_s^2 \propto A^{\frac{1}{3}}$ . For gold the saturation scale  $Q_{s,Au} \simeq 1.5 \text{ GeV}$  at  $x = 10^{-3}$ . Such a large value leads to considerable contribution of the high density QCD phase to RHIC data and reveals itself in essential damping for both  $xG_A$  and  $F_{2A}$ .

---

\*e-mail: leving@post.tau.ac.il

†e-mail: mal@techunix.technion.ac.il

# 1 Introduction

Deep inelastic scattering on nuclei gives us a new possibility to reach a high density QCD phase without requiring extremely low values of  $x$  (extremely high energies). This can be seen directly from simple estimates of the packing factors for the partons in DIS on nuclei. Indeed, the packing factor is equal to

$$\begin{aligned}
 \kappa_A(x, Q^2) &= \frac{3\alpha_S \pi^2}{Q^2} \times \frac{1}{\pi R_A^2} \times x G_A^{DGLAP}(x, Q^2) \\
 &= \frac{3\alpha_S \pi^2}{Q^2} \times \frac{1}{\pi R_A^2} \times A x G_N^{DGLAP}(x, Q^2) \\
 &\approx A^{\frac{1}{3}} \kappa_N(x, Q^2)
 \end{aligned} \tag{1.1}$$

For a gold nucleus the packing factor is the same as for a nucleon at  $x_A \approx 200 \cdot x_N$ , assuming  $x G_N(x, Q^2) \propto (1/x)^\lambda$  with  $\lambda \sim 0.3$  which follows from the HERA experimental data [1]. The gluon density  $x G^{DGLAP}$  is the solution of the linear DGLAP evolution equation [2]. The equation (1.1) implies another advantage of nuclear targets. Namely, the value of the saturation scale is larger for nuclear targets than for nucleon ones. Indeed, the simplest estimate for the saturation scale can be deduced from the equation  $\kappa_A(x, Q_{s,A}^2(x)) = 1$ . The solution of this equation is

$$Q_{s,A}^2(x) \propto A^{\frac{1}{3(1-\gamma)}} , \tag{1.2}$$

where the anomalous dimension  $\gamma = d \ln(x G_N) / d \ln Q^2$  is a smooth function of  $x$  and  $Q^2$ . The fact that the saturation scale is larger for nuclei from the theoretical point of view makes our calculations more reliable.

Determination of the saturation scale  $Q_{s,A}(x)$  is one of the most challenging problems in QCD. The DGLAP equation [2] describes the gluon radiation which increases the number of partons. However, when the parton density becomes large the annihilation processes enter the game and they suppress the gluon radiation. These effects tame the rapid increase of the parton densities at the saturation scale  $Q_{s,A}(x)$  [3, 4, 5]. At this scale the nonlinear effects become important and the parton evolution cannot be described by a linear equation any more. This argument stimulated a development of new methods [3, 4, 5, 6, 7, 8, 9, 10, 11, 13, 14, 15, 16], which finally lead to the very same nonlinear evolution equation for the imaginary part of the DIS elastic amplitude<sup>1</sup>:

$$N_A(\mathbf{x}_{01}, Y; b) = N_A(\mathbf{x}_{01}, Y_0; b) \exp \left[ -\frac{2 C_F \alpha_S}{\pi} \ln \left( \frac{\mathbf{x}_{01}^2}{\rho^2} \right) (Y - Y_0) \right] +$$

---

<sup>1</sup> Eq. (1.3) was proposed in momentum representation by Gribov, Levin and Ryskin [3] and it was proved in double log approximation of perturbative QCD by Mueller and Qiu [4], in Wilson Loop Operator Expansion at high energies by Balitsky [11], in colour dipole approach [12] to high energy scattering in QCD by Kovchegov [13], in effective Lagrangian approach for high parton density QCD by Iancu, Leonidov and McLerran (see Ref. [14] and Refs. [10] for previous efforts). Braun [16] derived this equation by summing ‘‘fan’’ diagrams, as GLR did, but using the triple BFKL ladder vertex of Refs. [17]. Therefore, this equation is a reliable tool for an extrapolation of the parton distributions to the region of low  $x$ .

$$\frac{C_F \alpha_S}{\pi^2} \int_{Y_0}^Y dy \exp \left[ -\frac{2 C_F \alpha_S}{\pi} \ln \left( \frac{\mathbf{x}_{01}^2}{\rho^2} \right) (Y - y) \right] \times \quad (1.3)$$

$$\int_{\rho} d^2 \mathbf{x}_2 \frac{\mathbf{x}_{01}^2}{\mathbf{x}_{02}^2 \mathbf{x}_{12}^2} \left( 2 N_A(\mathbf{x}_{02}, y; \mathbf{b} - \frac{1}{2} \mathbf{x}_{12}) - N_A(\mathbf{x}_{02}, y; \mathbf{b} - \frac{1}{2} \mathbf{x}_{12}) N_A(\mathbf{x}_{12}, y; \mathbf{b} - \frac{1}{2} \mathbf{x}_{02}) \right).$$

The equation is written for  $N_A(r_{\perp}, x; b) = \text{Im} a_{\text{dipole}}^{el}(r_{\perp}, x; b)$ , where  $a_{\text{dipole}}^{el}$  is the amplitude of the elastic scattering for the dipole of the size  $r_{\perp}$ . The total dipole cross section is given by

$$\sigma_{\text{dipole}}^A(r_{\perp}, x) = 2 \int d^2 b N_A(r_{\perp}, x; b). \quad (1.4)$$

The total deep inelastic cross section is related to the dipole cross section

$$\sigma_A(x, Q^2) = \int d^2 r_{\perp} \int dz |\Psi^{\gamma^*}(Q^2; r_{\perp}, z)|^2 \sigma_{\text{dipole}}^A(r_{\perp}, x), \quad (1.5)$$

where the QED wave functions  $\Psi^{\gamma^*}$  of the virtual photon are well known [12, 18, 19]. The equation (1.5) is quite transparent and it describes two stages of DIS [20]. The first one is the decay of a virtual photon into colourless dipole ( $q\bar{q}$ -pair) which is described by the wave function  $\Psi^{\gamma^*}$  in Eq. (1.5). The second stage is the interaction of the dipole with the target ( $\sigma_{\text{dipole}}^A$  in Eq. (1.5)). This equation is the simplest manifestation of the fact that the correct degrees of freedom at high energies in QCD are colour dipoles [12].

In the equation (1.3), the rapidity  $Y = -\ln x$  and  $Y_0 = -\ln x_0$ . The ultraviolet cutoff  $\rho$  is needed to regularize the integral, but it does not appear in physical quantities. In the large  $N_c$  (number of colours) limit  $C_F = N_c/2$ . Eq. (1.3) has a very simple meaning: the dipole of size  $\mathbf{x}_{10}$  decays into two dipoles of sizes  $\mathbf{x}_{12}$  and  $\mathbf{x}_{02}$  with the decay probability given by the wave function  $|\Psi|^2 = \frac{\mathbf{x}_{01}^2}{\mathbf{x}_{02}^2 \mathbf{x}_{12}^2}$ . These two dipoles then interact with the target. The non-linear term takes into account the Glauber corrections for such an interaction.

The equation (1.3) does not depend on the target explicitly. This independence is a direct indication that the equation is correct for any target in the regime of high parton density. The only dependence on a target comes from initial conditions at some initial value  $x_0$ . For a nucleus target it was proven in Refs. [7, 13] that the initial conditions should be taken in the Glauber form:

$$N_A(\mathbf{x}_{01}, x_0; b) = N_{GM}^A(\mathbf{x}_{01}, x_0; b), \quad (1.6)$$

with

$$N_{GM}^A(\mathbf{x}_{01}, x; b) = 1 - \exp \left[ -\frac{\sigma_{\text{dipole}}^N(r_{\perp}, x)}{2} S_A(b) \right]. \quad (1.7)$$

The cross section of the dipole interaction with a nucleon is defined as

$$\sigma_{\text{dipole}}^N(r_{\perp}, x) = 2 \int d^2 b N_N(r_{\perp}, x; b)$$

with  $N_N$  that has been calculated in the Ref. [21]. The equation (1.7) represents the Glauber - Mueller (GM) formula which accounts for the multiple dipole-target interaction in the eikonal approximation [18, 22, 23].

It turns out, however, that at sufficiently high initial  $x_0$  ( $x_0 \approx 10^{-2}$ ) the equation (1.7) leads to the same initial profile  $N_A$  as the simplified version

$$N_{GM}^A(\mathbf{x}_{01}, x; b) = 1 - \exp \left[ -\frac{\alpha_S \pi^2 \mathbf{x}_{01}^2}{2 N_c} x G^{DGLAP}(x, 4/\mathbf{x}_{01}^2) S_A(b) \right]. \quad (1.8)$$

The nucleon gluon distribution inside a nucleus  $x G^{DGLAP}$  is parameterized according to LO solution of the DGLAP equation [2]. The function  $S_A(b)$  is a dipole profile function inside the nucleus with the atomic number  $A$ . The value of  $x_0$  is chosen within the interval

$$\exp\left(-\frac{1}{\alpha_S}\right) \leq x_0 \leq \frac{1}{2mR_A}, \quad (1.9)$$

where  $R_A$  is the radius of the target. In this region the value of  $x_0$  is small enough to use the low  $x$  approximation but the production of the gluons (colour dipoles) is still suppressed since  $\alpha_S \ln(1/x) \leq 1$ . Therefore in this region we have instantaneous exchange of the classical gluon fields. Due to this fact an incoming colour dipole interacts separately with each nucleon in a nucleus [9].

Solutions to the equation (1.3) were studied in asymptotic limits in the Refs. [8, 15, 24, 25]. A first attempt to estimate numerically the value of the shadowing corrections in DIS on nuclei in the framework of the non-linear evolution equation was made in the Ref. [7]. In that paper the AGL evolution equation was solved in the semi-classical approximation. It turns out that the AGL equation is the same as Eq. (1.3) in the double log approximation but it is written not for the amplitude  $N$  but for the opacity  $\Omega$  ( $N = 1 - \exp(-\Omega/2)$ ). Braun [16] solved numerically an equation similar to Eq. (1.3) in momentum representation with some specific initial conditions and we will discuss his results below. In our recent paper [21] we solved Eq. (1.3) numerically for the proton targets.

Our approach to the solution of Eq. (1.3) is based on space representation. We have several arguments for working in this representation. First of all, it allows us to formulate the initial conditions. Moreover, the initial conditions are not known at large distances at all. Consequently we would expect problems calculating the amplitude in the momentum representation since it implies knowledge of the amplitude in the whole kinematic region of  $r_\perp$ . Our last argument is that in the space representation the unitarity constraints have the simplest form:

$$2 N(r_\perp, x; b) = N^2(r_\perp, x; b) + G_{in}(r_\perp, x; b), \quad (1.10)$$

where  $G_{in}$  stands for contributions of all inelastic processes. We assume in Eq. (1.10) that at high energies the elastic amplitude is dominantly imaginary  $a^{el}(r_\perp, x; b) \rightarrow N(r_\perp, x; b)$ . The equation (1.10) implies  $N(x, r_\perp; b) \leq 1$  with a natural limit  $N(x, r_\perp; b) \rightarrow 1$  at  $x \rightarrow 0$ . This limit provides us with a very useful check in our numerical approach.

In the present paper we report on our solution of the equation (1.3) for the nuclear targets. The method of iterations proposed in [21] is applied. Contrary to the Ref. [16] we study solutions for phenomenologically reasonable kinematic regions only, and for real nuclei. The main goal of the

research is determination of the saturation scale  $Q_{s,A}(x)$  and its dependence on the target atomic number  $A$ . We also present estimates of the gluon density  $xG_A$  and the structure function  $F_{2A}$  in the region of the high parton density QCD.

The paper is organized as follows. In the next section (2) we give a review of the nuclear target properties. In section 3 a solution of the nonlinear equation is presented. Section 4 is devoted to the calculations of  $xG_A$  and  $F_{2A}$ . In section 5 we determine the saturation scales and study their  $A$ -dependence. Section 6 presents discussion of the self-consistency of the numerical procedure and results. We conclude in the last section (7).

## 2 Nuclear input data

In this section we discuss the properties of the nuclei our computations are made for. The nuclei are described by their radial nucleon distribution  $\rho(r)$ . This distribution is normalized to the total nucleon number  $A$ :

$$\int \rho(r) d^3r = A. \quad (2.11)$$

The nucleon distribution for all nuclei discussed in this paper are parameterized by one of the following three parameterizations:

1. Two-parameter Fermi model (2pF)

$$\rho(r) = \rho_0 / (1 + \exp((r - c)/z)).$$

2. Three-parameter Fermi model (3pF)

$$\rho(r) = \rho_0 (1 + w r^2/c^2) / (1 + \exp((r - c)/z)).$$

3. Three-parameter Gaussian model (3pG)

$$\rho(r) = \rho_0 (1 + w r^2/c^2) / (1 + \exp((r^2 - c^2)/z^2)).$$

The constants  $c$ ,  $z$ , and  $w$  are free parameters varying from nucleus to nucleus. The table (1) lists the relevant input data for all nuclei used in this work [26]. The parameter  $\rho_0$  is always found due to the normalization (2.11).

The radius  $r$  can be decomposed to the transverse  $b$  and longitudinal  $r_l$  components

$$r^2 = b^2 + r_l^2.$$

Then the transverse profile function  $S_A(b)$  is defined as the integral of the radial density  $\rho$  over the longitudinal component  $r_l$ :

$$S_A(b) = \int \rho(r) dr_l. \quad (2.12)$$

Fig. 1 displays the function  $S_A(b)$  for various nuclei.

Nucleus	$A$	model	$R_A$ [fm]	$c$ [fm]	$z$ [fm]	$w$
<i>Ne</i>	20	2pF	3	2.805	0.571	
<i>Ca</i>	40	3pF	3.486	3.6685	0.5839	-0.1017
<i>Zn</i>	70	2pF	4.044	4.409	0.583	
<i>Mo</i>	100	3pG	4.461	4.559	2.6723	0.339
<i>Nd</i>	150	2pF	5.048	5.7185	0.651	
<i>Au</i>	197	2pF	5.33	6.38	0.535	

**Table 1:** Parameters for the nucleon distributions in the nuclei taken from the Ref. [26].

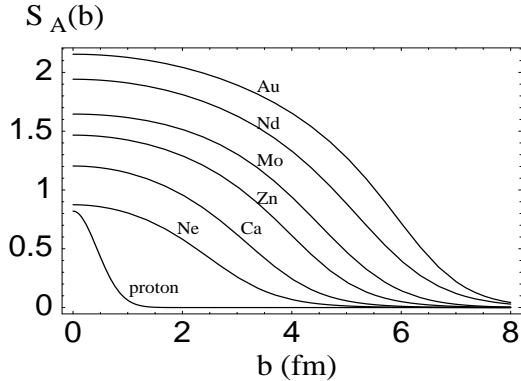


**Figure 1:** The nucleon transverse profile function inside the nucleus  $S_A(b)$  is plotted as a function of  $b$ .

We wish to draw reader's attention to the fact that  $S(b=0)$  for proton is almost the same as for *Ne* (see Fig. 1). This fact has an obvious explanation: partons inside the proton are distributed in smaller area with  $R \approx 3 \text{ GeV}^{-1} = 0.6 \text{ fm}$  which is smaller than the area given by extrapolation of the Wood-Saxon parameterization to  $A = 1$ . Indeed,  $R_{A=1} \simeq 1.2 \text{ fm} > R = 0.6 \text{ fm}$ . This simple fact makes our estimates based on Eq. (1.1) too optimistic. We will show below that the packing factor for gold is the same as for nucleon at  $x_{Au} \approx (5 \div 10) \cdot x_N$ .

### 3 Solution of the nonlinear equation

In the Ref. [21] we suggested to solve the equation (1.3) by the method of iterations. All details about our method can be found in that paper, where the equation (1.3) was solved numerically for the proton target.

Following the very same procedure as in [21] we obtain numerical solutions for all nuclei listed above. For  $xG^{DGLAP}(x, Q^2)$  we use the GRV'94 parameterization and the leading order solution of the DGLAP evolution equation [27]. The initial conditions (1.6) are set at  $x_0 = 10^{-2}$ . The constant value for the strong coupling constant  $\alpha_S = 0.25$  is always used. The solutions are computed within the kinematic region down to  $x = 10^{-7}$  and distances up to a few fermi.

The function  $N_A$  is formally a function of three variables: the energy variable  $x$ , the transverse distance  $r_\perp$ , and the impact parameter  $b$ . The  $b$ -dependence is parametric only because the

evolution kernel does not depend on  $b$ . In order to simplify the problem we assume that the function  $N_A$  preserves the very same  $b$ -dependence as introduced in the initial conditions:<sup>2</sup>

$$N_A(r_\perp, x; b) = (1 - e^{-\kappa_A(x, r_\perp) S_A(b)/S_A(0)}). \quad (3.13)$$

The function  $\kappa_A$  is related to the “ $b = 0$ ” solution  $\tilde{N}_A(r_\perp, x)$ :

$$\kappa_A(x, r_\perp) = -\ln(1 - \tilde{N}_A(r_\perp, x)). \quad (3.14)$$

$\tilde{N}_A(r_\perp, x)$  represents a solution of the very same equation (1.3) but with no dependence on the third variable. The initial conditions for the function  $\tilde{N}_A(r_\perp, x)$  are taken at  $b = 0$ . For the case of the proton target [21] the ansatz in the form (3.13) is shown to be a quite good approximation of the exact  $b$ -dependence of the solution to (1.3). We will investigate the accuracy of this ansatz for gold in the end of this section.

For each nucleus the function  $\tilde{N}_A(r_\perp, x)$  is obtained after about ten iterations. The Fig. 2 shows the solutions for various nuclei. Note that though the solutions are of similar form they differ from each other indicating some memory of the initial conditions.

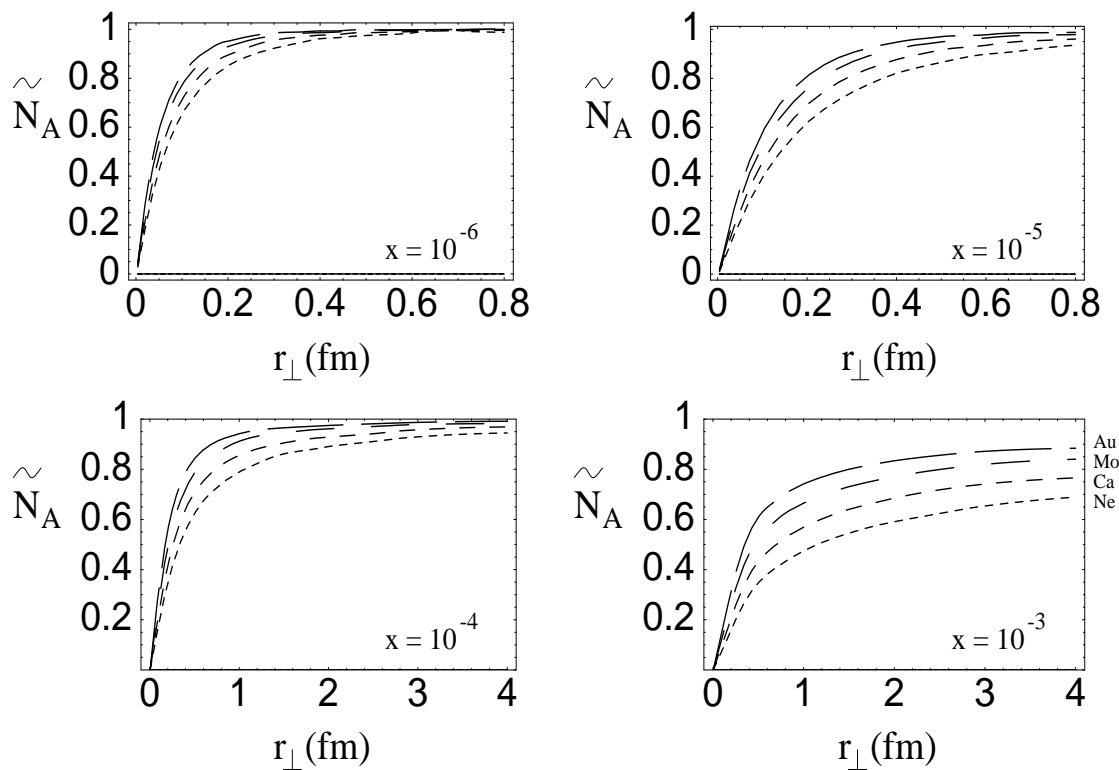


**Figure 2:** The function  $\tilde{N}_A$  is plotted versus distance. The four curves show the result for the nuclei *Ne*, *Ca*, *Mo*, and *Au*.

It is worth to compare the obtained solutions with the Glauber formula (1.8). For example the comparison is made for two nuclei: the lightest one *Ne* and the most heavy *Au*. The two models are plotted together in the figure 3.

<sup>2</sup>Note that for the Gaussian parameterization of the profile function  $S_A$ ,  $A = \pi R_A^2 S_A(0)$ .

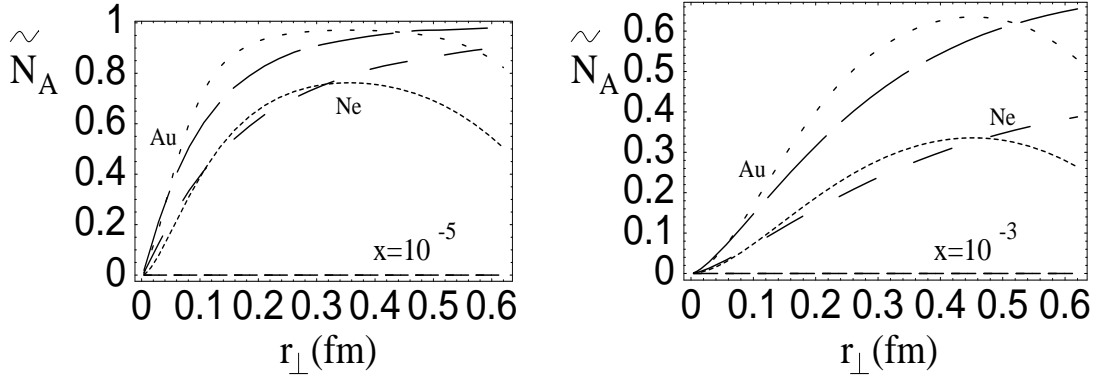


**Figure 3:** The functions  $\tilde{N}_A$  for Au and Ne (dashed lines) are plotted together with the corresponding Glauber formulas (dotted lines).

Having obtained the solutions for nuclei we can answer the question about the energetic gain of performing DIS on nuclei. To this goal the results for nuclei should be compared with ones for proton targets [21]. Unfortunately, the gain is quite modest and it consists of about half order of magnitude for very heavy nuclei. Namely, for a gold target *Au* the scattering amplitude  $\tilde{N}_{Au}$  (and consequently the packing factor  $\kappa_{Au}$ ) almost coincides with the proton one when  $x_{Au} \simeq 5 x_{proton}$ , which is quite different from the previous optimistic estimates (see Eq. (1.1) and discussion there). The simple reason for such a mild gain was mentioned in the previous section and it is related to the fact that  $S_N(b=0)$  is almost the same as for *Ne* as can be seen in the Fig. 1.

It is possible to determine the gluon density  $xG_A$  from the solutions obtained. To this goal the accuracy of the ansatz (3.13) has to be estimated. The  $b$ -dependence so far ignored in the function  $\tilde{N}_A$  should be investigated. In order to restore the  $b$ -dependence of the function  $N_A$  we solve the equation (1.3) with the only assumption that the impact parameter  $b$  is much larger than the dipole sizes:

$$\mathbf{x}_{01} \ll b; \quad \mathbf{x}_{02} \ll b. \quad (3.15)$$

In this case the  $b$ -dependence of the rhs of (1.3) is significantly simplified. We perform the computations for only one nucleus *Au*, which is the most different from the proton among the nuclei that we have considered. The Fig. 4 shows examples of the comparison between the correct  $b$ -dependence of the solution and the ansatz (Eq. (3.13)). It can be seen from the figure Fig. 4 that our ansatz (3.13) is a very good approximation for relatively small  $b$  and up to  $b \sim R_A$ . For larger impact parameters our ansatz underestimates the true solution. This fact can be simply understood theoretically. At very large impact parameters the exponential in (3.13) can be expanded and we get  $N_A = \kappa_A S(b)/S(0)$ . Then substitution of the ansatz to the equation (1.3) shows that it underestimates the solution indeed. For such values of the impact parameter it is more natural to search for the true solution of (1.3) in the form  $N_A(r_\perp, x; b) = n_A(r_\perp, x) S(b)/S(0)$  and to write down an evolution equation directly for the function  $n_A$ . In this case, we would obtain the function  $n_A$  somewhat larger than our  $\kappa_A$ . Such an approach was adopted in the Ref. [28] but for the whole range in  $b$  which seems to be wrong for small impact parameters and the Glauber initial conditions (1.6).

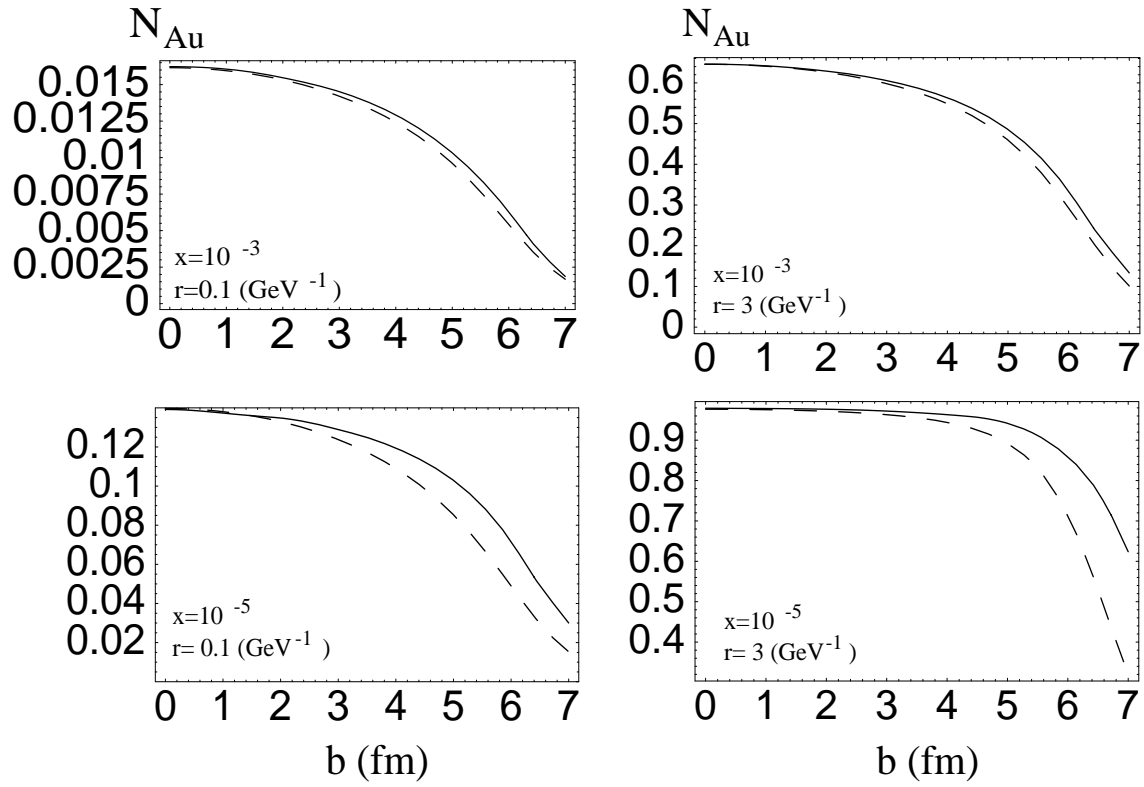


**Figure 4:** The function  $N_{Au}$  is plotted versus the impact parameter  $b$ . The solid line is the exact  $b$  dependence, while the dashed line is the ansatz (3.13).

## 4 Gluon density and the $F_2$ structure function

### 4.1 Gluon density $xG_A$

We can proceed now with the computation of the gluon density  $xG_A$  which we define using the Mueller formula [18]:

$$xG_A(x, Q^2) = \frac{4}{\pi^3} \int_x^1 \frac{dx'}{x'} \int_{4/Q^2}^\infty \frac{dr^2}{r^4} \int d^2b 2 N_A(r, x'; b). \quad (4.16)$$

There is some uncertainty in (4.16) due to  $b$ -integration. Supposing that the main contributions to the  $b$ -integration come from the region  $b \sim R_A$ , the uncertainty can be estimated. In this region the ansatz (3.13) underestimates the solution by maximum about 25%, and hence the obtained gluon density is also expected to be underestimated by the same amount. The Fig. 5 presents results of the calculations for the gluon density  $xG_A$  for three values of  $Q^2$  while the Fig. 6 shows its  $Q^2$  dependence for various  $x$ .

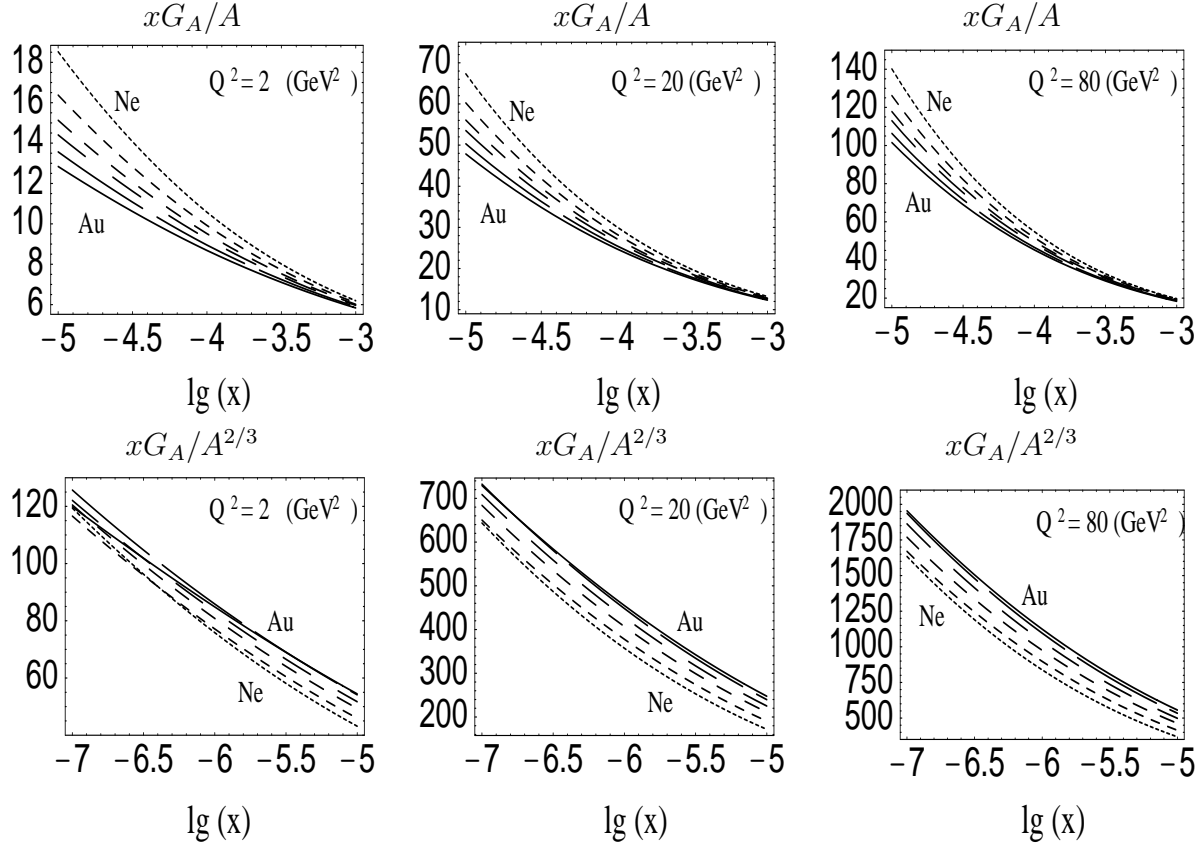


**Figure 5:** The gluon density  $xG_A$  is plotted as a function of  $\lg x$  for the nuclei Ne, Ca, Zn, Mo, Nd, and Au.

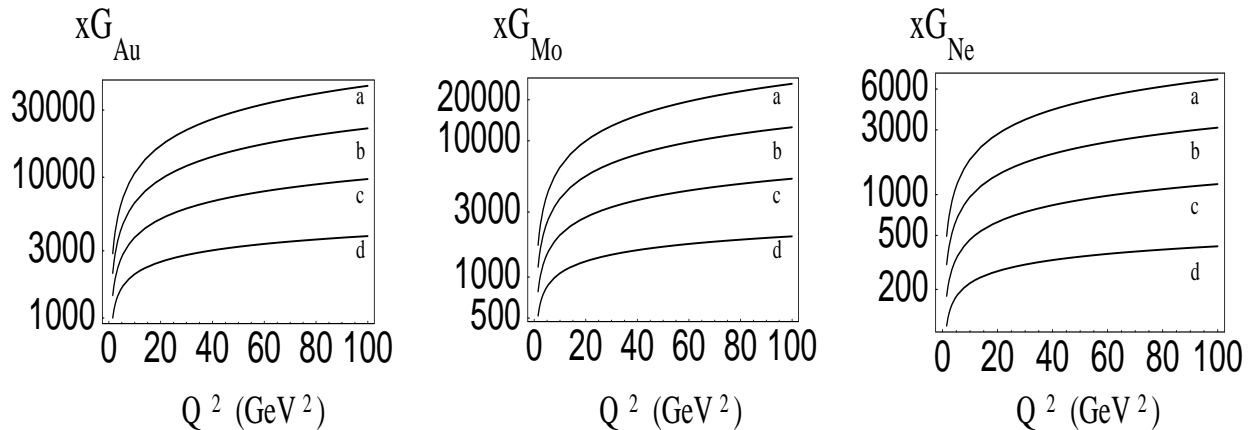


**Figure 6:** The gluon density  $xG_A$  is plotted as a function of  $Q^2$ ; a -  $x = 10^{-6}$ ; b -  $x = 10^{-5}$ ; c -  $x = 10^{-4}$ ; d -  $x = 10^{-3}$ .

$Q^2 \setminus x$	$10^{-7}$	$10^{-6}$	$10^{-5}$	$10^{-4}$	$10^{-3}$
$2 \text{ GeV}^2$	0.73	0.78	0.84	0.92	0.97
$15 \text{ GeV}^2$	0.74	0.79	0.85	0.92	0.97
$40 \text{ GeV}^2$	0.75	0.8	0.86	0.92	0.97
$120 \text{ GeV}^2$	0.76	0.81	0.87	0.92	0.97

**Table 2:** The power  $n$  for various values of  $x$ .

The gluon density  $xG_A$  defined as in (4.16) grows with decreasing  $x$ . In a sense, this observation contradicts the “super-saturation” of Ref. [16] where the density is predicted to vanish in the large rapidity limit. However, the gluon density definition accepted in Ref. [16] differs from ours, and hence the functions are not compatible.

It is important to investigate the  $A$  dependence of the gluon density  $xG_A$ . The leading twist perturbative QCD prediction based on DGLAP equation is  $xG_A = AxG_N$ , where  $xG_N$  is a nucleon gluon density.

Let parameterize the  $A$  dependence as  $xG_A = A^n xG_N$ . The results obtained for the power  $n$  are presented in the table (2). At high  $x$  we indeed obtain the law  $xG_A \simeq AxG_N$  which is shown in the Fig. 5. At moderate  $x \simeq 10^{-5}$  a transition occurs and  $n$  turns out to be quite different from 1. At low  $x$  the gluon density  $xG_A$  is rather proportional to  $A^{2/3}$  (Fig. 5). For large  $Q^2$  the transition occurs at somewhat smaller  $x$ , but the dependence on  $Q^2$  is very weak (Table 2). This described  $A$  dependence is actually anticipated from general theoretical arguments (see Ref. [7] and references therein).

## 4.2 Anomalous dimension

We define the average anomalous dimension as follows [7]:

$$\gamma(A, x, Q^2) = \frac{d(\ln xG_A(x, Q^2))}{d \ln Q^2}. \quad (4.17)$$

The results of the computations are presented on the Fig. 7-a. To our surprise the anomalous dimension almost does not depend on the atomic number  $A$  displaying independence on the target. However, the anomalous dimension for the function  $\tilde{N}_A$  satisfying Eq. (1.3) shows a considerable  $A$  dependence as can be seen in the Fig. 7 (b-c). We define

$$\gamma_N = \frac{d \ln \tilde{N}_A(2/Q, x)}{d \ln Q^2} + 1 .$$

Such a different behavior of  $\gamma$  and  $\gamma_N$ , in our opinion, is mostly related to the fact that shorter distances enter the calculation of  $\gamma$  compared to  $\gamma_N$  as can be observed directly from Eq. (4.17).

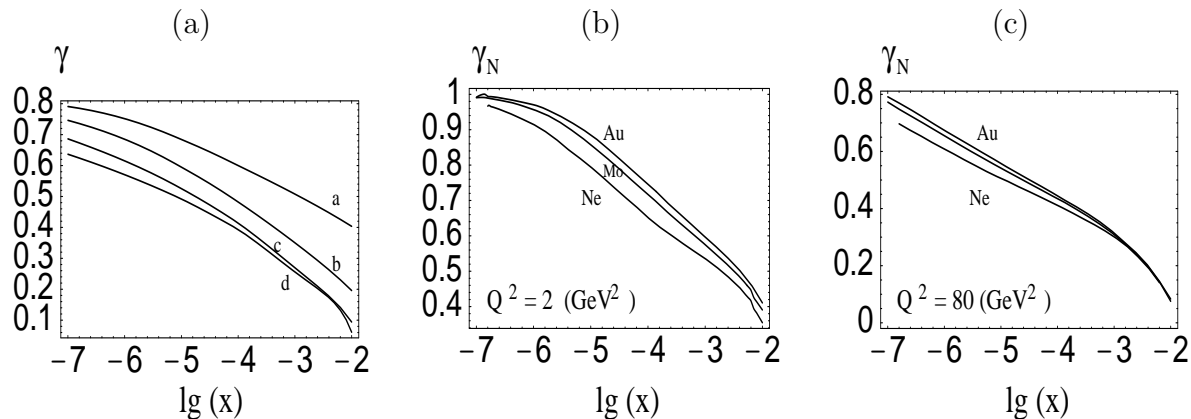


**Figure 7:** The anomalous dimensions are plotted as a function of  $\lg x$ . (a) -  $\gamma$  for the various values of  $Q^2$ : a -  $1.5 \text{ GeV}^2$ , b -  $5 \text{ GeV}^2$ , c -  $30 \text{ GeV}^2$ , d -  $120 \text{ GeV}^2$ ; (b) -  $\gamma_N$  for  $Q^2 = 2 \text{ GeV}^2$ ; (c) -  $\gamma_N$  for  $Q^2 = 80 \text{ GeV}^2$ .

### 4.3 $F_{2A}$

The structure function  $F_{2A}$  is related to the dipole cross section

$$F_{2A}(x, Q^2) = \frac{2}{\pi^3} \int_{4/Q^2}^{\infty} \frac{dr^2}{r^4} \int d^2b N_A(r, x; b). \quad (4.18)$$

The Fig. 8 presents the function  $F_{2A}$  for various nuclei.

We now in the position when we can try to compare our results with ones obtained in the Ref. [16]. That paper presents results for the structure function  $F_2$  computed for the lead nuclei ( $A = 207$ ). Unfortunately, the kinematic regions investigated in our work and in the Ref. [16] have a very small overlap. Nevertheless at not extremely low  $x$  and not too high  $Q^2 \leq 1000 \text{ GeV}^2$  a comparison can be made (we use our gold ( $A = 197$ ) calculations). We fail to reproduce results of the Ref. [16]. In all the region of the comparison we predict a few times smaller values for the function  $F_{2A}$ .

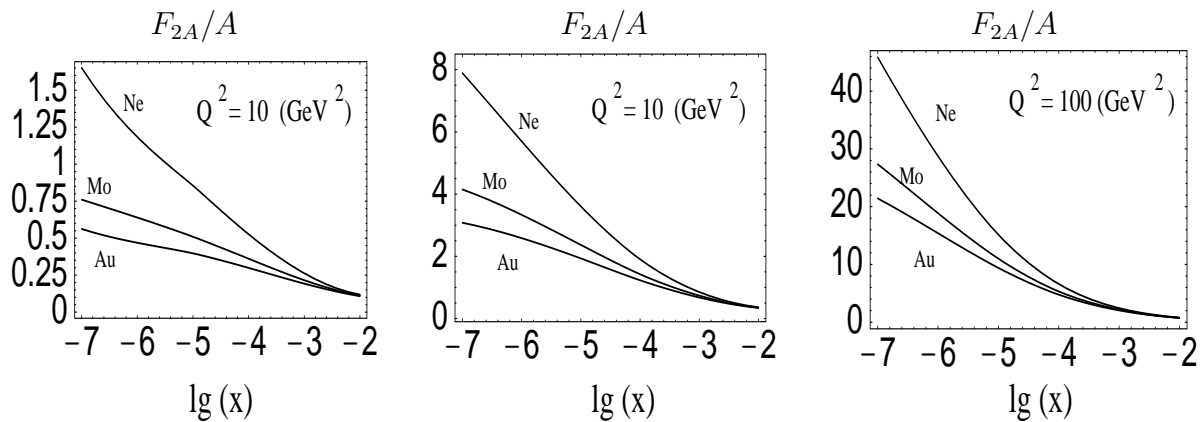


**Figure 8:** The structure function  $F_{2A}/A$  is plotted as a function of  $\lg x$  for the nuclei Au, Mo, and Ne.

There are several reasons for the obtained mismatch. First of all, there are few minor ones related to the difference between the nuclei compared and different  $\alpha_s$  used in the computations. In addition, our treatments of the  $b$ -dependence are quite different. However, in our opinion, the main reason is in the initial conditions of the evolution, which do not coincide with the ones of the Ref. [16]. At moderate  $x$  ( $x = 10^{-3} \div 10^{-5}$ ) our solution depends on initial condition as well as at lower  $x$  where such a dependence is concentrated at very short distances.

Concluding this comparison we would like to make the following comment. We actually believe that our results on  $F_{2A}$  are more reasonable. At not very low  $x \simeq 10^{-2} \div 10^{-4}$  we expect the function  $F_{2A}$  to be proportional to  $A$ . Namely,  $F_{2A} \simeq A F_2$ . Our results on  $F_{2A}$  display this behavior and are in a good agreement with the experimental data on the proton structure function  $F_2$ . Contrary to us, the results of [16] seem to be few times off from this agreement.

## 5 Saturation

It is natural to define the saturation scale through the equation

$$\kappa_A(x, 2/Q_s) = 1/2. \quad (5.19)$$

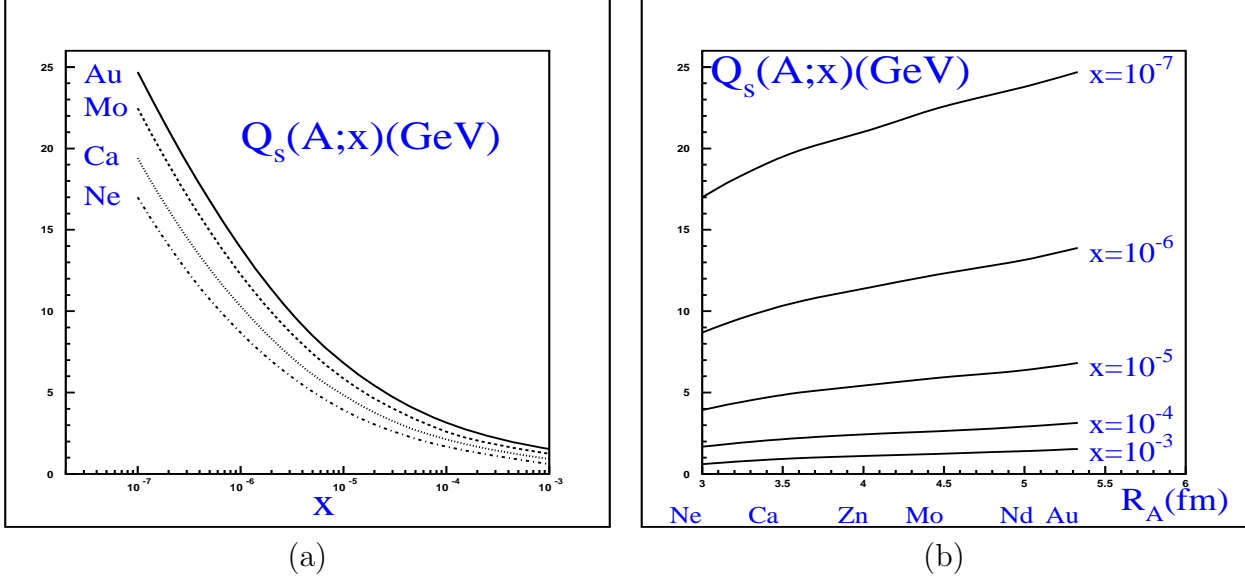
The definition (5.19) agrees with the one adopted for the Glauber formula (1.8).

Fig. 9 displays the saturation scale  $Q_{s,A}$  obtained in (5.19) for various nuclei.

The main question which we want to study is the dependence of the saturation scale  $Q_{s,A}(x)$  on the atomic number  $A$ . Let us assume a power law behavior for the saturation scale  $Q_{s,A}(x)$  as a function of  $A$ :

$$Q_{s,A}(x) = C(x) A^{p(x)}, \quad (5.20)$$

where  $C(x)$  and  $p(x)$  are  $x$  dependent functions. The power  $p(x)$  is of our main interest. In order to check the ansatz (5.20) and find the power we study the  $A$  dependence of the saturation scale in double logarithmic scale and find it to fit well a straight line that justifies use of the ansatz



**Figure 9:** The saturation scale  $Q_{s,A}$  is plotted versus  $\lg x$  (a) and  $R_A$  (b).

Nuclei \ $x$	$10^{-7}$	$10^{-6}$	$10^{-5}$	$10^{-4}$	$10^{-3}$
Light	0.18	0.22	0.26	0.31	0.49
Heavy	0.15	0.19	0.22	0.24	0.31
All	0.17	0.20	0.24	0.27	0.39

**Table 3:** The power  $p(x)$  for various values of  $x$ .

(5.20). The power  $p(x)$  can be found by the least square fit. The table (3) presents the fit for the three cases: light nuclei ( $Ne, Ca, Zn$ ); heavy nuclei ( $Zn, Mo, Nd$ , and  $Au$ ); all nuclei together.

The table (3) is quite transparent. The power  $p(x)$  decreases with decreasing  $x$ . At the beginning of the evolution the  $A$ -dependence of the saturation scale for the light nuclei is close to the law  $Q_{s,A} \sim A^{1/2}$ , at  $x \simeq 10^{-4}$  the saturation scale  $Q_{s,A} \sim A^{1/3}$ , while at higher energies it tends to  $Q_{s,A}^2 \sim A^{1/3}$ . For the heavy nuclei the situation is similar but the decrease of the power  $p(x)$  is significantly slower. The above observations are in complete contradiction with conclusions derived in the Ref. [25], where the saturation scales were deduced from the equation (1.3) in the double logarithmic approximation. The main source of this large discrepancy is the fact that the anomalous dimension in the solution of the DGLAP equation turns out to be larger than  $1/2$  which is the maximum value for the BFKL evolution in the leading order (see Eq. (1.2)). This is a disturbing result since it could mean that the leading order non-linear evolution equation (see Eq. (1.3)) is not enough to make a reliable predictions in the kinematic region of high density QCD.

We would like to stress that the numbers presented in the table (3) are quite approximate. These numbers display a certain sensitivity to the definition of the saturation scale (we use Eq. (5.19) but other definitions can be investigated as well). Moreover, the powers obtained are results of regressions over too small number of points, which actually implies large errors. However, we are convinced that the decreasing property of the power  $p(x)$  with high energies is quite general.

Table (3) can be explained qualitatively in terms of the anomalous dimension  $\gamma$ . The following arguments are presented for the GM formula (Eq. (1.8)) or/and for the packing factor (Eq. (1.1)), but the physical picture is valid for the solution of the equation (1.3) as well. In the GM formula the power  $p(x) = \frac{1}{6(1-\gamma)}$ . Though  $\gamma$  is usually assumed to be small, it is often not the case. Moreover,  $\gamma$  is actually  $x$  and  $Q$  dependent. At large  $x$  and correspondingly small saturation scale  $Q_{s,A}$  the GRV gluon density parameterization implies very large  $\gamma$  tending to unity (see e.g. Ref. [7]). This is the origin of the large powers in the table (3). When we go from light nuclei to more heavy (at fixed  $x$ ) the saturation scale obtained increases, and consequently  $\gamma$  decreases. That is why smaller powers are obtained for the heavy nuclei compared to the light ones. As  $x$  decreases, on one hand  $\gamma$  increases at fixed  $Q$ . On the other hand, at smaller  $x$  a larger saturation scale  $Q_{s,A}$  is obtained. Finally, with decreasing  $x$  the power  $p(x)$  decreases as well tending to the value  $p(x) = \frac{1}{6}$ .

## 6 Discussion of the results

Let us explain qualitatively the  $A$  dependence of the results. We also wish to perform checks for the self-consistency of the results obtained.

The main starting observation is that the anomalous dimension  $\gamma$  (4.17) is almost  $A$  independent while its  $Q^2$  dependence become weaker as  $x$  decreases.

Define the power  $\alpha$ :

$$\alpha(A, x, Q^2) = - \frac{d(\ln \kappa_A(x, 2/Q))}{d \ln Q^2}. \quad (6.21)$$

We find that  $\alpha \simeq 1 - \gamma$ . Consequently we can try to write  $\kappa_A$  in the power-like form:

$$\kappa_A(x, r_\perp) \sim A^{\beta(x)} (r_\perp^2)^\alpha. \quad (6.22)$$

In the equation (6.22) we introduced the  $A$ -dependence in order to define the saturation scale:

$$Q_{s,A}(x) \sim A^{\beta/(2\alpha)} = A^{p(x)}. \quad (6.23)$$

The power  $\beta$  is obtained to be almost  $Q^2$  independent. It ranges from about 0.33 at  $x = 10^{-3}$  and to about 0.17 at  $x = 10^{-7}$ . Meanwhile at the saturation scale  $\alpha$  is almost constant  $\alpha \simeq 0.45 \div 0.5$ . This corresponds to  $\gamma \simeq 0.5$ , which is the anomalous dimension of the linear BFKL term in the nonlinear equation (1.3).

Assuming  $\kappa_A$  be relatively small we would obtain for the gluon density

$$xG_A(x, Q^2) \sim R_A^2 \int_x^1 \frac{dx'}{x'} \int_{4/Q^2} \frac{dr^2}{r^4} \kappa_A(x', r). \quad (6.24)$$

Substituting (6.22) to the equation (6.24) we obtain

$$xG_A(x, Q^2) \sim R_A^2 \int_x^1 \frac{dx'}{x'} (Q^2)^{1-\alpha} A^\beta. \quad (6.25)$$

Assuming that the integral in (6.25) is dominated by  $x' \simeq x$ , we see that within the above approximation  $\gamma \simeq 1 - \alpha$  indeed. The independence of the anomalous dimension on  $A$  is a consequence of the fact that  $\beta$  happened to be almost  $Q^2$  independent.

What about  $A$ -dependence of the gluon density? We obtain for the power  $n$  the relation

$$n(x) = 2/3 + \beta(x) = 2/3 + 2p(x)\alpha(x). \quad (6.26)$$

The equation (6.26) is in a sense an additional consistency check. The numbers presented in the tables (2) and (3) are in a good agreement with each other (though the equation (6.26) is not fulfilled exactly due to many approximations done on the way to (6.26)). The fact that the powers  $n$  in the table (2) do not much sensitive to  $Q^2$  is now understood as a consequence of the corresponding independence of  $\beta$ .

## 7 Conclusions

In this paper we reported on the exact numerical solutions of the nonlinear evolution equation (1.3) for nuclear targets. The solutions are obtained by the method of iterations proposed in the Ref. [21]. Various nuclei starting from the very light  $Ne_{20}$  and up to heavy  $Au_{197}$  were investigated.

We demonstrated that the solution to the non-linear equation is quite different from the GM model that has been used for estimates of the saturation effects. However, this model can be used as a first iteration of the non-linear equation which leads to faster convergence of the numerical procedure.

From the experimental point of view the obtained results support the energetic profit for performing DIS experiments on nuclei. However, the gain is quite modest, and it can be estimated about five times for gold targets compared with proton.

The gluon density  $xG_A$  and the structure function  $F_{2A}$  were estimated. At small  $x \simeq 10^{-6} \div 10^{-7}$  the damping due to non-linear effects leads to suppression of a factor  $2 \div 4$  for heavy nuclei in comparison with the DGLAP prediction  $xG_A = AxG^{DGLAP}$ . At moderate  $x \simeq 10^{-2} \div 10^{-4}$  the structure function  $F_{2A} \simeq AF_2$ , where the obtained values for  $F_2$  agree well with the experimental data on proton.

The dependence of the gluon density  $xG_A$  was investigated as a function of the atomic number  $A$ . At high  $x$ , the density is shown to be proportional to  $A$ . A transition occurs at moderate  $x \simeq 10^{-4}$ . At small  $x$ ,  $xG_A$  is rather proportional to  $A^{2/3}$ . To our knowledge this is a first numerical confirmation of this dependence from the master equation Eq. (1.3) expected on general grounds.

The found solutions of the nonlinear equation were used to estimate the saturation scale  $Q_{s,A}(x)$ . In agreement with all theoretical predictions the saturation scale grows with decreasing  $x$ .

The dependence of the saturation scales on the atomic number  $A$  was a focus of the research. A fit of the saturation scale to the power law  $Q_{s,A}(x) \sim A^{p(x)}$  was investigated. The numerical values obtained for the power  $p(x)$  are actually sensitive to the saturation scale definition. Nevertheless, we predict a decreasing behavior of the power with decreasing  $x$  for both heavy and light nuclei.

One of the interesting properties of the solutions of the equation (1.3) is that they display the scaling phenomena. Namely, the solution  $\tilde{N}_A$  is not a function of two variables  $x$  and  $r_\perp$  but rather a function of a single variable  $r_\perp Q_{s,A}(x)$ . A complete report on this subject is now in a final stage of preparation and will appear shortly [30].

Among several observations which come from the numerical solutions we would like to point out that the weak dependence of  $xG_A$  anomalous dimension on the atomic numbers as well as the fact that  $Q_{s,A}^2 \propto A^{1/3}$  at  $x \rightarrow 0$  look quite impressive for us. They certainly need some theoretical explanation and we hope they will stimulate such explanations. We firmly believe that our calculations of  $Q_{s,A}$  for various nuclei will provide a theoretical basis for the discussion of the RHIC data in high parton density QCD approach [29].

When the present paper was finished for publication we read a new paper [31] devoted to the very same subject. We have to stress that the initial conditions of our analyses are quite different. Though within the evolution in  $x$  the influence of initial conditions become weaker they are important for quantitative analysis in the experimentally reasonable region of not too small  $x$ . We were pleased to discover that despite the difference in the initial conditions the saturation scale  $Q_s$  obtained in [31] is proportional to  $A^{2/9}$ , which is a dependence quite similar to ours. The scaling phenomena confirmed by the numerical calculations of the Ref. [31] has been also observed by one of us and the report will appear soon [30].

### Acknowledgments :

We are very grateful to Ia. Balitsky, M. Braun, E. Gotsman, E. Iancu, D. Kharzeev, Yu. Kovchegov, U. Maor, L. McLerran and K. Tuchin for illuminating discussions on the subject.

This research was supported in part by the BSF grant # 9800276, by the GIF grant # I-620-22.14/1999 and by Israeli Science Foundation, founded by the Israeli Academy of Science and Humanities.

## References

- [1] A. M. Cooper-Sarkar, R. C. E. Devenish and A. De Roeck, *Int. J. Mod. Phys. A* **13** (1998) 33;  
H. Abramowicz and A. Caldwell, *Rev. Mod. Phys.* **71** (1999) 1275.
- [2] V. N. Gribov and L. N. Lipatov, *Sov. J. Nucl. Phys* **15** (1972) 438; G. Altarelli and G. Parisi, *Nucl. Phys. B* **126** (1977) 298; Yu. I. Dokshitzer, *Sov. Phys. JETP* **46** (1977) 641.

- [3] L. V. Gribov, E. M. Levin, and M. G. Ryskin, *Phys. Rep.* **100** (1981) 1.
- [4] A. H. Mueller and J. Qiu, *Nucl. Phys.* **B 268** (1986) 427.
- [5] L. McLerran and R. Venugopalan, *Phys. Rev.* **D 49** (1994) 2233, 3352; **D 50** (1994) 2225, **D 53** (1996) 458, **D 59** (1999) 094002.
- [6] L. V. Gribov, E. M. Levin, and M. G. Ryskin, *Nucl. Phys.* **B 188** (1981) 555;  
E. Levin and M.G. Ryskin, *Phys. Rep.* **189** (1990) 267;  
J. C. Collins and J. Kwiecinski, *Nucl. Phys.* **B 335** (1990) 89;  
J. Bartels, J. Blumlein, and G. Shuler, *Z. Phys.* **C 50** (1991) 91;  
E. Laenen and E. Levin, *Ann. Rev. Nucl. Part. Sci.* **44** (1994) 199 and references therein;  
Yu. Kovchegov, *Phys. Rev.* **D 54** (1996) 5463, **D 55** (1997) 5445, **D 61** (2000) 074018.
- [7] A. L. Ayala, M. B. Gay Ducati, and E. M. Levin, *Nucl. Phys.* **B 493** (1997) 305, **B 510** (1998) 355.
- [8] A. H. Mueller, *Nucl. Phys.* **B 572** (2000) 227, **B 558** (1999) 285.
- [9] Yu. V. Kovchegov, A. H. Mueller, *Nucl. Phys.* **B 529** (1998) 451.
- [10] J. Jalilian-Marian, A. Kovner, L. McLerran, and H. Weigert, *Phys. Rev.* **D 55** (1997) 5414; J. Jalilian-Marian, A. Kovner, and H. Weigert, *Phys. Rev.* **D 59** (1999) 014015; J. Jalilian-Marian, A. Kovner, A. Leonidov, and H. Weigert, *Phys. Rev.* **D 59** (1999) 034007, Erratum-ibid. *Phys. Rev.* **D 59** (1999) 099903; A. Kovner, J. Guilherme Milhano, and H. Weigert, *Phys. Rev.* **D 62** (2000) 114005, H. Weigert, “Unitarity at small Bjorken  $x$ ”, NORDITA-2000-34-HE, hep-ph/0004044.
- [11] Ia. Balitsky, *Nucl. Phys.* **B 463** (1996) 99.
- [12] A. H. Mueller, *Nucl. Phys.* **B 415** (1994) 373.
- [13] Yu. Kovchegov, *Phys. Rev.* **D 60** (2000) 034008.
- [14] E. Iancu, A. Leonidov, and L. McLerran, “Nonlinear gluon evolution in the color glass condensate”, BNL-NT-00/24, hep-ph/0011241.
- [15] E. Iancu and L. McLerran, “Saturation and Universality in QCD at small  $x$ ”, Saclay-T01-026, hep-ph/0103032.
- [16] M. Braun, *Eur. Phys. J.* **C 16** (2000) 337; “High energy interaction with nucleus in the perturbative QCD with  $N_c \rightarrow \infty$ ”, hep-ph/0101070.
- [17] A. Mueller and B. Patel, *Nucl. Phys.* **B 425** (1994) 471;  
J. Bartels and M. Wuesthoff, *Z. Phys.* **C 66** (1995) 157.
- [18] A. H. Mueller, *Nucl. Phys.* **B 335** (1990) 115.

- [19] N. N. Nikolaev and B. G. Zakharov, *Z. Phys. C* **49** (1991) 607; E. M. Levin, A. D. Martin, M. G. Ryskin, and T. Teubner, *Z. Phys. C* **74** (1997) 671.
- [20] V. N. Gribov, *Sov. Phys. JETP* **30** (1970) 709.
- [21] M. Lublinsky, E. Gotsman, E. Levin, and U. Maor, “*Non-linear evolution and parton distributions at LHC and THERA energies*”, TAUP - 2667 - 2001, hep-ph/0102321.
- [22] A. Zamolodchikov, B. Kopeliovich, and L. Lapidus, *JETP Lett.* **33** (1981) 595.
- [23] E. M. Levin and M. G. Ryskin, *Sov. J. Nucl. Phys.* **45** (1987) 150.
- [24] Yu. Kovchegov, *Phys. Rev. D* **61** (2000) 074018;
- [25] E. Levin and K. Tuchin, *Nucl. Phys. B* **573** (2000) 833; “*New scaling at high energy DIS*”, hep-ph/0012167; “*Nonlinear evolution and saturation for heavy nuclei in DIS*”, hep-ph/0101275.
- [26] C. W. De Jagier, H. De Vries, and C. De Vries, *Atomic Data and Nuclear Data Tables* **Vol. 14** No 5, 6 (1974) 479.
- [27] M. Gluck, E. Reya, and A. Vogt, *Eur. Phys. J. C* **5** (1998) 461.
- [28] M. A. Kimber, J. Kwiecinski, and A. D. Martin, “*Gluon shadowing in the low  $x$  region probed by the LHC*”, IPPP-01/01, DCPT/01/02, hep-ph/0101099.
- [29] N. Armesto and C. Pajares, *Int. J. Mod. Phys. A* **15** (2000) 2019, hep-ph/0002163; A. Krasnitz and R. Venugopalan, *Phys. Rev. Lett.* **86** (2001) 1717; “*Nonperturbative gluodynamics of high energy heavy ion collision*”, hep-ph/0004116; *Phys. Rev. Lett.* **84** (2000) 4309; K. J. Eskola, K. Kajantie, P. V. Ruuskanen and K. Tuominen, *Nucl. Phys.* **570** (2000) 379 and references therein; K. J. Eskola, K. Kajantie and K. Tuominen, *Phys. Lett. B* **497** (2001) 39; K. J. Eskola, P. V. Ruuskanen, S. S. Rasanen and K. Tuominen, “*Multiplicities and transverse energies in central AA collisions at RHIC and LHC from pQCD, saturation and hydrodynamics*”, JYFL-3-01, hep-ph/0104010; D. Kharzeev and M. Nardi, “*Hadron production in nuclear collisions at RHIC and high density QCD*”, nucl-th/0012025.
- [30] M. Lublinsky, “*Scaling phenomena from non-linear evolution in high energy DIS*”, in preparation.
- [31] N. Armesto and M. Braun, “*Parton densities and dipole cross-sections at small  $x$  in large nuclei*”, hep-ph/0104038.